Biochemistry 1993, *32*, 1180–1187

Probing the Combining Site of an Anti-Carbohydrate Antibody by Saturation–Mutagenesis: Role of the Heavy-Chain CDR3 Residues

David A. Brummell,[‡] Vidhya P. Sharma, Naveen N. Anand,[§] Doris Bilous, Ginette Dubuc, Joseph Michniewicz, C. Roger MacKenzie, Joanna Sadowska, Bent W. Sigurskjold,[∥] Barbara Sinnott, N. Martin Young, David R. Bundle, and Saran A. Narang*

Institute for Biological Sciences, National Research Council of Canada, Ottawa, Ontario K1A 0R6, Canada

Received July 17, 1992; Revised Manuscript Received October 7, 1992

ABSTRACT: The carbohydrate-binding site in Fab fragments of an antibody specific for *Salmonella* serogroup B O-polysaccharide has been probed by site-directed mutagenesis using an *Escherichia coli* expression system. Of the six hypervariable loops, the CDR3 of the heavy chain was selected for exhaustive study because of its significant contribution to binding-site topography. A total of 90 mutants were produced and screened by an affinity electrophoresis/Western blotting method. Those of particular interest were further characterized by enzyme immunoassay, and on this basis seven of the mutant Fabs were selected for thermodynamic characterization by titration microcalorimetry. With regard to residues that hydrogen bond to ligand through backbone interactions, Gly^{102H} could not be substituted, while several side chains could be introduced at Gly^{100H} and Tyr^{103H} with relatively little effect on antigen binding. There was, however, a preference for nonpolar side chains at position 103H. Substitution of His^{101H} with carboxylate and amide side chains gave mutants with binding affinities approaching that of the wild type; complete side-chain removal by mutation to Gly was tolerated with a 10-fold reduction in binding constant. Analysis of binding by titration microcalorimetry revealed some dramatic thermodynamic changes hidden by the similarity of the binding constants. Similar effects were observed with residue changes in an Arg-Asp salt-bridge at the base of the loop. These results indicate that alterations to higher affinity anti-carbohydrate antibodies are characterized by an enthalpy–entropy compensation factor which allows for fundamental changes in the nature of the binding interactions but impedes engineering for increases in affinity.

As evidence for the crucial role of carbohydrates as recognition elements in cellular functions increases, so does the desirability of gaining a full understanding of how the biological roles of carbohydrates are exerted through their interactions with proteins (Vyas, 1991). A recent increase in the number of well-refined structures has provided considerable insight into the atomic interactions at play in these processes. In our laboratory, the details of carbohydrate binding by antibodies have, for the first time, been described at atomic resolution. The crystal structure of a Fab complexed with a *Salmonella* O-antigen of serogroup B has been solved at 2.05-Å resolution (Cygler et al., 1991). The antigen, built from the four-sugar repeating unit

$$\{\rightarrow 2)[\alpha\text{D-Abe}^{1}(1\rightarrow 3)]\alpha\text{D-Man}(1\rightarrow 4)\alpha\text{L-Rha}(1\rightarrow 3)\alpha\text{D-Gal}(1\rightarrow\}$$

is bound in a "pocket"-like site via a network of hydrogen bonds and van der Waals contacts (Figure 1). Abequose, the immunodominant sugar, is totally buried, while mannose and galactose residues lie on the protein surface and are partially exposed to water.

We have initiated a protein engineering study of the combining site of the anti-*Salmonella* antibody to test the various site residues and to complement antigen analog studies. Such detailed analyses of well-defined protein–carbohydrate structures are necessary to understand the principles governing the relationship among structure, specificity, and affinity in carbohydrate recognition systems. Without this type of information, strategic and astute redesign of carbohydrate binding sites will be difficult. Structure–function studies by site-directed mutagenesis have to date been confined to sugar-binding proteins from the bacterial periplasm (Quiocho, 1991; Vermersch et al., 1990, 1991). As a model system for this type of study, the *Salmonella* antibody offers several advantages in addition to the well-refined crystal structure. These include a detailed description of binding thermodynamics (Sigurskjold et al., 1991; Sigurskjold & Bundle, 1992) and an efficient *Escherichia coli* expression system (Anand et al., 1990, 1991a) that yields active product through the use of bacterial signal peptides (Better et al., 1988; Skerra & Plückthun, 1988). With a binding constant of 2×10^5 M^{-1}, the anti-*Salmonella* antibody has very good affinity for an anti-carbohydrate antibody.

Antibody binding sites are constructed chiefly from six segments, three from each chain, termed CDRs. The origin of the CDR-H3 from the D-segment of the gene together with junctional and N-diversity (Alt & Baltimore, 1982) leads to far greater sequence variation in this CDR than in the other five. As often occurs in antibodies (Alzari et al., 1988; Mian et al., 1991), the heavy-chain CDR3 of the *Salmonella* antibody makes a greater contribution to antigen binding than do the other five CDR loops. Four of the eight residues that form hydrogen bonds to the antigen reside in this loop (Figures 1 and 2). Another feature of the H3 loop is the presence at

* Author to whom correspondence should be addressed [telephone (613) 990-3247; fax (613) 941-1327].

‡ Present address: Department of Vegetable Crops, Mann Laboratory, University of California, Davis, CA 95616-8631.

§ Present address: Connaught Laboratories Ltd., Willowdale, ON, Canada.

∥ Present address: Department of Chemistry, Carlsberg Laboratory, DK-2500 Copenhagen Valby, Denmark.

[⊥] Abbreviations: Abe, 3,6-dideoxy-*xylo*-hexose; BSA, bovine serum albumin; CDR, complementary-determining region; EIA, enzyme immunoassay; H3, heavy-chain CDR3; PVDF, poly(vinylidene fluoride).

0006-2960/93/0432-1180$04.00/0 Published 1993 by the American Chemical Society

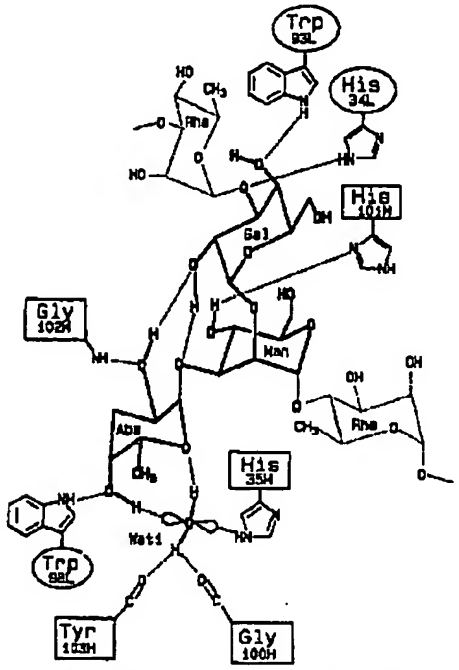

FIGURE 1: Details of Se155-4 CDR-H3 involvement in binding the trisaccharide epitope of *Salmonella* serogroup B O-antigen: hydrogen-bonding scheme highlighting H3 residue (in boxes) involvement.

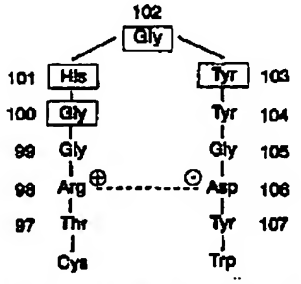

FIGURE 2: Heavy-chain CDR3 sequence indicating the residues (in boxes) which hydrogen-bond to antigen and the position of the Arg^{98H}–Asp^{106H} salt-bridge.

its base of a salt-bridge (Chothia & Lesk, 1987) which may stabilize its conformation (Figure 2). In other antibodies alterations to this salt-bridge gave unpredictable and interesting results (Chien et al., 1989; Novotny et al., 1990; Panka et al., 1988). For these reasons, our combining site engineering studies have focused on H3. In this paper we describe the results of mutagenesis of each of the four H3 contact residues into each of the other 19 amino acid side chains. Such a systematic approach may lead to a better appreciation of the role of this key CDR in the formation of the antigen binding site.

EXPERIMENTAL PROCEDURES

Materials. Restriction enzymes and DNA-modifying enzymes were purchased from New England Biolabs and Bethesda Research Laboratories. All DNA manipulations were carried out essentially as described by Sambrook et al. (1989). Oligonucleotides were synthesized on an Applied Biosystems Model 380A automatic DNA synthesizer. Enzyme conjugates and substrates for immunoassays were obtained from Caltag, Kirkegaard and Perry Laboratories and Bio-Rad.

Fab Gene Construction. The dicistronic Fab construct pSal–Fab (Anand et al., 1991a) consisting of the Fd and light chain genes, each preceded by the *ompA* signal peptide, in the expression plasmid pUCE8 (Narang et al., 1987) was modified somewhat prior to the initiation of this study. An unpaired cysteine (Cys^{94L}) was mutated to Ser, using the codon TCT, to eliminate unwanted disulfide bond formation. This change had no detectable effect on antigen binding as measured by enzyme immunoassay (data not shown). Also, a single base pair error at heavy-chain residue 65 (AGT, encoding Ser, instead of the required CGT, encoding Arg) was corrected. This was accomplished by replacing the *PflMI* (Thr^{30H}) to *SpeI* (Thr^{74H}) segment with six synthetic oligonucleotides, at the same time changing the GAG Glu^{46H} codon to GAA, thus destroying the *XhoI* site at Leu^{45H}, and changing the CGT Arg^{40H} codon to CGG, thereby generating an *EagI* site. The corrected plasmid was designated pSal–FabB. The pSal–FabB product had an affinity for antigen that was approximately 50% better than that of the Ser^{45H} mutant (pSal–Fab product).

Generation of Mutants. Site-directed mutagenesis was carried out by a double-mutation approach (Narang et al., 1991). For heavy-chain substitutions between positions 100H and 106H, pSal–FabB was cut at the unique *MluI* (at Thr^{97H}) and *SacI* (at Ser^{117H}) sites and the *MluI–SacI* segment was replaced in each cloning with four synthetic oligonucleotides (Figure 3). In each instance, the left-hand pair of oligonucleotides possessed one to three mismatches which introduced the codon for one substitution on the top strand and the anticodon for the second substitution on the bottom strand. The right-hand pair of oligonucleotides was common for each cloning and possessed a single silent mismatch at position 112H, with the result that clones derived from the top strand gained an extra *KasI* site and clones derived from the bottom strand gained an extra *NheI* site. These restriction sites were used to screen miniprep DNA prior to sequencing. A similar procedure was employed to generate mutants in the 97H–99H and 106H–107H regions, except that a unique *BsgI* site (recognition sequence at 95H, cut site a 90H) was used instead of *MluI* and the junction between the two pairs of oligonucleotides was moved five amino acids to the left. In all cases nucleotide sequences were confirmed by sequencing with the dideoxy method using the Sequenase kit (U.S. Biochemicals Corp.).

Expression and Isolation of Mutant Fabs. E. coli, strain TG-1, harboring wild-type or mutant pSal–FabB plasmid was grown with shaking at 30 °C in M9 medium supplemented with 0.4% (w/v) casamino acids and 5 mg/L thiamin, in the presence of 100 mg/L ampicillin. At 24 h, cultures were induced by adding supplementary nutrients (12 g of tryptone, 24 g of yeast extract, and 4 mL of glycerol per liter) and 1 mM isopropyl thiogalactopyranoside. After a further 66 h of growth, active Fab was isolated from periplasmic extracts by affinity chromatography as described previously (Anand et al., 1991a).

Affinity Electrophoresis. An affinity electrophoresis method using acrylamide gels containing antigen was developed on the basis of principles originally described by Takeo and coworkers (Takeo & Nakamura, 1972; Takeo & Kabat, 1978). Native polyacrylamide gels were made for the PhastSystem (Pharmacia). Separating gels were 8% acrylamide in 112 mM Tris acetate buffer, pH 6.4, and stacking gels were 3% acrylamide in 56 mM Tris acetate buffer, pH 6.4. For ligand-

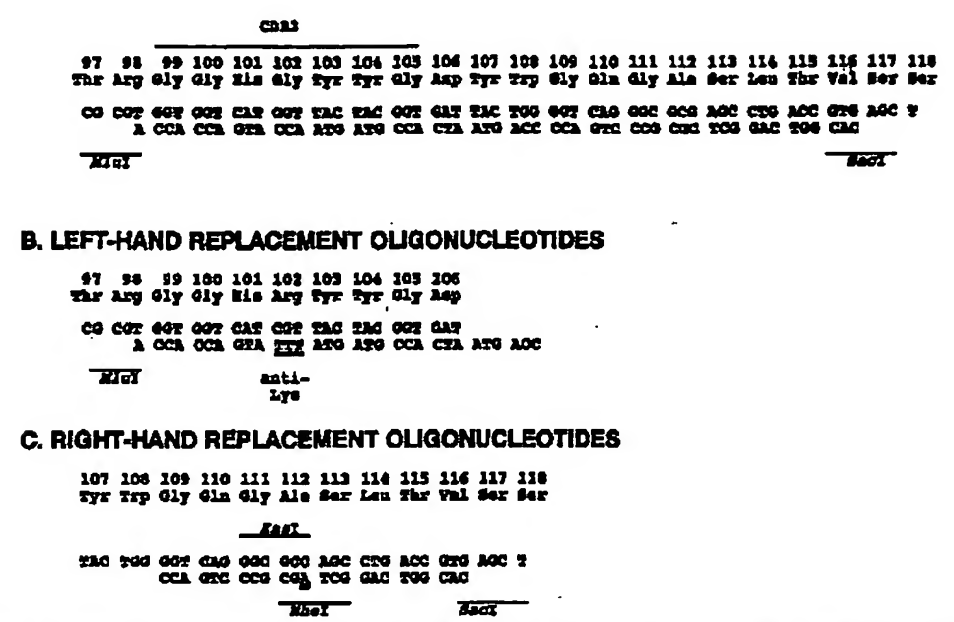

FIGURE 3: Cloning procedure for the generation of CDR-H3 mutants. The wild-type sequence (A) was replaced by four oligonucleotides: two left-hand oligos (B) encoding the desired mutations and two right-hand oligos (C) that introduced a *KasI* site in clones derived from the top strand and an *NheI* site in clones derived from the bottom strand. The same right-hand oligos were used in all clonings. In this example, position 102H is changed to arginine (and gains a *KasI* restriction site) or lysine (and gains an *NheI* restriction site). Mismatches are double-underlined.

containing gels, *Salmonella* serogroup B O-antigen prepared from *Salmonella essen* lipopolysaccharide (Svenson & Lindberg, 1978) was added to separating gel mixtures to 0.005% (w/v) prior to polymerization. This antigen concentration would give at least at 50-fold excess of antigen over antibody in gels, assuming a Fab production level of 20 mg/L of bacterial culture, and meets the requirements described by Takeo and Kabat (1978). Native buffer strips were obtained from Pharmacia. Fab samples were electrophoresed in gels with and without antigen at 10 mA for 268 Vh as recommended by Pharmacia for native gels. Following electrophoresis, Western blots were made simply by placing the gel in contact with PVDF membrane (Millipore) that had been wetted in methanol and soaked in 25 mM Tris–192 mM glycine, pH 8.4. The contact time was 2 min with three consecutive blots being taken from the same gel. The blots were developed with an anti-mouse lambda-chain–alkaline phosphatase conjugate (Caltag). The second and third blots from each gel generally gave less background staining. The distances to which Fab bands migrated in the presence and absence of antigen were measured from the blots. The degree to which wild-type Fab migration was retarded by antigen

$$(d - d_{Ag})/d$$

where d is the distance migrated in the absence of antigen and d_{Ag} the distance in the presence of antigen, was assigned a value of 1, and values for mutant Fab retardation relative to that of the wild-type were calculated.

Binding Assays. Following preliminary screening by affinity electrophoresis, the antigen-binding properties of mutants of particular relevance were further investigated by indirect EIA. These assays were carried out as described previously (Anand et al., 1991b) using microtiter plates coated with BSA–O-polysaccharide conjugate (E. Altman, unpublished results).

The binding thermodynamics of selected mutants were determined by titration microcalorimetry using an OMEGA titration microcalorimeter (Wiseman et al., 1989) from Microcal Inc. (Northampton, MA). Wild-type and mutant Fabs, at concentrations of approximately 50 μM in 50 mM Tris and 150 mM NaCl, pH 8.0, were titrated with a 2 mM solution of synthetic trisaccharide antigen in the same buffer at 25 °C. The ligand solution was injected in 20 portions of 5 μL. Thermogram data were analyzed as described previously (Sigurskjold et al., 1991; Sigurskjold & Bundle, 1992).

RESULTS

Targeting H3 Mutations. The H3 loop of Se155-4 consists of nine residues (99H–107H, sequential numbering system). Four of these residues, all from the D-region, form hydrogen bonds with the bound trisaccharide (Figures 1 and 2). The loop is also characterized by a salt-bridge, at its base, between Arg^{98H} and Asp^{106H}. The loop is quite short compared to H3 loops in general and is characterized by a predominance of glycine and tyrosine residues, with Gly^{100H}, Gly^{102H}, and Tyr^{103H} forming hydrogen bonds to antigen and to a structured water molecule through NH and C=O groups of the main chain. Tyr^{103H} also contributes one of several aromatic side chains that define the binding site. His^{101H} accepts a hydrogen bond from O-4 of mannose and is one of three histidine residues participating in the hydrogen-bond network. Although His^{101H} is largely exposed to solvent (Figure 4), antigen mapping studies have shown that its interaction with mannose is important. These four D-region contact residues were targeted for site-directed mutagenesis because of their role in antigen binding and the fact that they are representative of the types of interactions that characterize carbohydrate binding by Se155-4. The role of the Arg^{98H}–Asp^{106H} salt-bridge in maintaining the integrity of the combining site was also probed

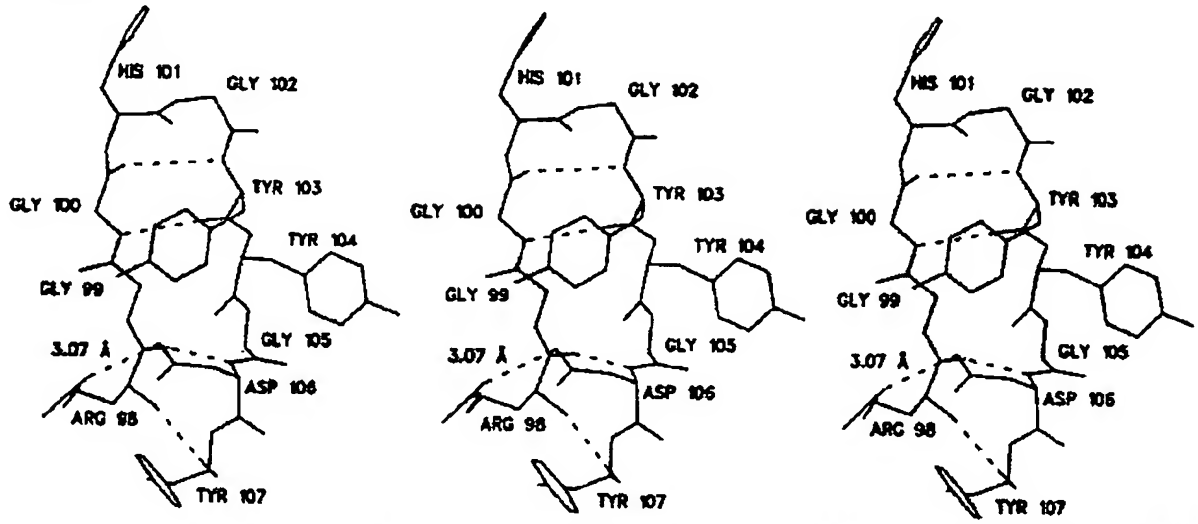

FIGURE 4: Stereoview of the wild-type heavy-chain CDR3 loop showing internal hydrogen bonds and the position of the Arg^{98H}–Asp^{106H} salt-bridge.

Table I: Affinity Electrophoresis Analysis of Antigen-Binding Activity of H3 Contact Residue Mutants[a]

changed to	Gly^{100H}	His^{101K}	Gly^{102H}	Tyr^{103H}
Ala	0.9	0.55	0.75	ND[b]
Arg	0.85	0.35	0.05	ND
Asn	0.9	0.9[c]	0.1	0.75
Asp	0.9	1.0[c]	0	0.5
Cys	ND	ND	ND	ND
Glu	1.0	0.85[c]	0.05	0.8
Gln	0.9	0.9[c]	0.1	0.8
Gly	1.0	0.85[c]	1.0	0.75
His	0.9	1.0	0.15	0.9
Ile	0.35	0.45	0.2	0.9
Leu	0.7	0.4	0.15	0.95
Lys	0.9	0.5	0.05	ND
Met	0.8	0.5	0.25	0.85
Phe	0.85	0.3	0.1	0.9
Pro	0.4	0.8	0.05	0.2
Ser	0.9	0.75	0.45	0.7
Thr	0.65	0.5	0.35	0.8
Trp	0.95	0.1	ND	0.9
Tyr	0.9	0.4	0.1	1.0
Val	0.05	0.55	0.05	0.9

[a] The values of relative retardation are given to ±0.05. [b] Fab band not detected. [c] Microcalorimetry also done.

by a limited number of amino acid substitutions. Both salt-bridge residues are partially buried and quite distant from the binding site (Figure 4).

Expression and Mutagenesis of Se155-4 Fab. Active Fab fragments with interchain disulfide bonds formed in good yield in the *E. coli* periplasm. The double-replacement mutagenesis technique provided an efficient means of mutant generation. Mutants identified by preliminary restriction-cut screening were confirmed to have the correct sequence 8 of 10 times. The wild-type construct gave 3–5 mg/L of active periplasmic product, but the yields of mutant Fabs were sometimes dramatically higher or lower. The five His^{101H} substitutions that gave the most active Fab molecules (Table I) had yields of 15–20 mg/L. In contrast, Western blotting indicated that introduction of cysteine residues into the loop resulted in poor yields of secreted product. Western blotting and Coomassie staining of affinity chromatography fractions showed that, for active mutants, all of the periplasmic Fab was fully active.

Affinity Electrophoresis. Mutant Fabs were screened for antigen-binding activity by an affinity electrophoresis/Western blotting technique developed specifically for this purpose. The procedure has the double advantage of screening simultaneously for periplasmic Fab presence and activity. In instances involving a change in molecular charge, the mutation is also confirmed by a mobility change in the native gels (Figure 5). The detection sensitivity was such that unconcentrated periplasmic extracts generally gave strong Fab bands using the standard assay conditions. As a screening method, the technique is considerably more accurate than previously used column procedures (Narang et al., 1991).

FIGURE 5: Affinity electrophoresis of wild-type and mutant Fabs. Western blots were prepared following the electrophoresis of identical samples in the absence (A) and presence (B) of *Salmonella* serogroup B O-antigen in the gel. The top of the separating gel is at the top of the photograph, and a free light-chain band is visible at the bottom of the gel in lane 3. 1, Wild-type; 2, $His^{101H}Asp$; 3, $His^{101H}Phe$; 4, $Asp^{104H}Tyr$-$Tyr^{107H}Asp$.

CDR Mutants. The 4 H3 residues that hydrogen bond to the oligosaccharide were mutated to all other 19 amino acids. Wild-type Fab controls were included as a check on techniques (Table I). Fab bands were readily detectable, by affinity electrophoresis, in periplasmic extracts of most mutants with

Table II: Relative Affinity for Antigen of Salt-Bridge Mutants As Estimated by Retardation during Affinity Electrophoresis[a]

	mutation[a]					retardation relative to wild type
	Thr^{97H}	Arg^{98H}	Gly^{99H}	Asp^{106H}	Tyr^{107H}	
1	–	Ala	–	–	–	0.2
2	–	–	–	Ala	–	0.85
3	–	–	–	Asn	–	0.9
4	–	Lys	–	–	–	1.0
5	–	–	–	Glu	–	0.95
6	–	Lys	–	Glu	–	1.0
7	–	Asp	–	Arg	–	0.3
8	–	–	–	Tyr	Asp	1.05
9	–	–	–	Tyr	Glu	ND[b]
10	–	Lys	–	Tyr	Asp	0.9
11	–	Lys	–	Tyr	Glu	0.95
12	Arg	Thr	–	–	–	0
13	–	Gly	Arg	–	–	ND

[a] Dashes denote wild-type amino acid. [b] Fab band not detected.

the notable exception of those involving the incorporation of a cysteine residue into the loop. The results indicated that none of the mutations resulted in improved affinity.

The affinity electrophoresis results showed that Gly^{100H}, which accepts a H-bond from the ordered water molecule, could be replaced by several amino acids without drastic loss of binding activity. On the basis of titration microcalorimetry data indicating that an affinity electrophoresis value of 0.85 represented a 10-fold drop in binding constant, approximately 60% of the mutants had affinities that were within an order of magnitude of that of the wild type. Surprisingly, very large side chains could be introduced without much effect; the activity of Gly^{100H}Trp, for example, resembled that of the wild type. On the other hand, any substitution of Gly^{102H} resulted in an enormous drop in activity. Results for the Tyr^{103H} position, at which the backbone C=O group accepts a H-bond from the ordered water molecule, indicated a preference for an alkyl/hydrophobic side chain, with such residues giving binding affinities within an order of magnitude of that of the wild type.

A more exhaustive study of the His^{101H} changes was undertaken to probe the histidine–sugar interactions that are so prominent in antigen binding by Se155-4. Introduction of hydrophobic side chains at this position virtually abolished binding. The best substitutions were aspartic acid, asparagine, glutamic acid, and glutamine. However, side-chain removal, i.e., His^{101H}Gly, was also tolerated to a remarkable degree. His^{101H}Pro and His^{101H}Ser were also moderately active. The five most active mutants as screened by affinity electrophoresis were selected for more in-depth analysis and were purified by affinity chromatography. Indirect EIA performed with the purified Fabs confirmed the affinity electrophoresis results, giving an activity ranking of His > Asp > Asn > Gln > Glu > Gly (data not shown).

Salt-Bridge Alterations. The construction of the various salt-bridge mutants and the affinity electrophoresis data obtained for them are presented in Table II. The results confirmed the requirement of a positively charged residue at position 98H and to a lesser degree the importance of a negatively charged residue at position 106H. While Arg^{98H}-Lys was fully active, Arg^{98H}Ala exhibited a complete loss of binding activity. The absolute requirement for positive charge at position 98H was further confirmed by the Thr^{97H}Arg and Arg^{98H}Thr double mutation. Glutamic acid was a good replacement for Asp at position 106H, but the requirement for a negative charge at this position was considerably less stringent since both Asp^{106H}Ala and Asp^{106H}Asn displayed relatively good activity. Of particular interest was the double mutant Asp^{106H}Tyr and Tyr^{107H}Asp, which displayed binding activity that was higher than that of the wild type. This was observed by affinity electrophoresis (Table II) and confirmed by indirect EIA, with the latter method indicating a 3-fold increase in activity (data not shown).

Titration Microcalorimetry. A thermodynamic analysis of the five most active His^{101H} mutants and the most active salt-bridge mutant was obtained by titration microcalorimetry (Table III). The results confirmed the reliability of the affinity electrophoresis technique as a screening procedure insofar as all five had K_a values of $\geq 2 \times 10^4\ M^{-1}$. At the His^{101H} position, an increase of over 50% in the enthalpy terms was observed for the Glu and Gln mutants. However, an opposing entropic effect precluded any increase in affinity. Affinities, in fact, were 3–4 times less than that of the wild type. This dramatic shift in thermodynamic parameters was not observed for the Asp and Asn mutants. With these mutants, ΔH° values were somewhat lower and ΔS° values relatively unchanged relative to those of the wild type. This indicated that these structural changes have little effect on binding chacteristics other than slightly weaker hydrogen bonding or van der Waals forces. The complete removal of the 101H side chain in the glycine mutant gives a molecule displaying a 10-fold lower affinity [$(2 \pm 0.5) \times 10^4\ M^{-1}$], a highly favorable enthalpy term and a highly unfavorable entropy term. Such a result is open to several interpretations, such as water-mediated hydrogen bonding or improved contacts provided by a more flexible H3 loop. The calorimetric data for the salt-bridge mutant in which the positions of Asp^{106H} and Tyr^{107H} were reversed indicated that binding by the double mutant was completely enthalpy driven with neither positive nor negative contribution from the entropy term. However, unlike the electrophoresis and indirect EIA results which indicated higher activity for the double mutant, the binding constant of the double mutant as determined by microcalorimetry [$(1.7 \pm 0.3) \times 10^5\ M^{-1}$] was the same as that of the wild type. Changing the salt-bridge partners to Lys and Glu resulted in a higher enthalpy term that was offset by an unfavorable entropy change.

DISCUSSION

Proteins that recognize carbohydrates must meet the unique challenge of discriminating among a vast number of sugar structures arising from the stereochemistry of hydroxyl groups in monosaccharides and different sugar linkage possibilities. Failure in this regard could be disastrous since carbohydrates are used as the recognition molecules in key cellular processes (Feizi, 1991). With a number of well-refined crystal structures of protein–carbohydrate complexes now solved (Quiocho, 1991; Vyas, 1991), some insight into how these strict requirements are met is being acquired. The atomic features of carbohydrate binding are best understood for the bacterial periplasmic receptors involved in sugar transport (Quiocho, 1991). With dissociation constants in the micromolar range, these proteins are at the upper end of the affinity spectrum for sugar-binding proteins. They are characterized by binding sites that are largely buried and solvent inaccessible, a stacking of aromatic residues against the sugar ring, and hydrogen bonding of sugar hydroxyls to polar amino acid side chains (Quiocho, 1991; Spurlino et al., 1991; Vyas et al., 1991). A considerable amount of information is also available on sugar binding by plant lectins and anti-carbohydrate antibodies (Bundle & Young, 1992). These proteins, characterized by affinities that are somewhat lower than those of the periplasmic receptors, have binding sites that are near the protein surface

Table III: Thermodynamic Parameters for Antigen Binding by Selected H3 Mutants of Se155-4

	K (M^{-1})	ΔG° (kJ mol^{-1})	ΔH° (kJ mol^{-1})	$-T\Delta S^\circ$ (kJ mol^{-1})
E. coli WT Fab	$(2.1 \pm 0.3) \times 10^5$	-30.3 ± 0.4	-24.8 ± 0.6	-5.5 ± 0.7
His^{101H}→Glu	$(3.7 \pm 1.0) \times 10^4$	-26.1 ± 0.7	-44.4 ± 5.5	18.3 ± 5.5
His^{101H}→Gln	$(7.6 \pm 2.1) \times 10^4$	-27.9 ± 0.7	-36.1 ± 3.0	8.2 ± 3.1
His^{101H}→Asp	$(7.1 \pm 1.5) \times 10^4$	-27.7 ± 0.5	-22.3 ± 1.2	-5.3 ± 1.3
His^{101H}→Asn	$(6.0 \pm 1.2) \times 10^4$	-27.2 ± 0.5	-23.1 ± 1.3	-4.2 ± 1.4
His^{101H}→Gly	$(2.0 \pm 0.5) \times 10^4$	-24.6 ± 0.6	-41.1 ± 5.5	16.6 ± 5.5
Arg^{98H}→Lys and Asp^{106H}→Glu	$(5.8 \pm 1.0) \times 10^4$	-27.2 ± 0.4	-39.3 ± 2.0	12.1 ± 2.1
Asp^{106H}→Tyr and Tyr^{107H}→Asp	$(1.7 \pm 0.3) \times 10^5$	-30.0 ± 0.4	-29.2 ± 1.0	-0.7 ± 1.1

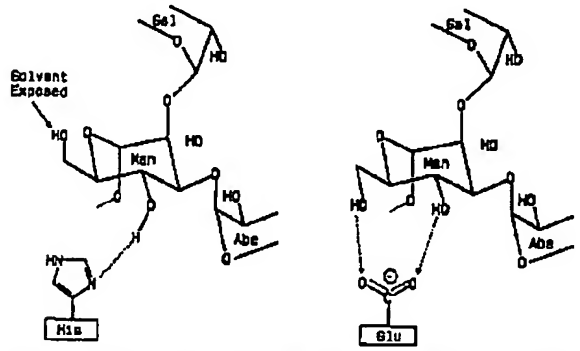

FIGURE 6: Postulated hydrogen-bond changes associated with His^{101H}→Glu mutation. The hydrogen-bonding scheme for O-4 of the mannose residue is shown for the native complex and for the His^{101H}Glu mutant. Although Glu is shown here, this potential bidentate hydrogen bonding to mannose O-4 and O-6 could be achieved with Asp, Asn, and Gln and might require the participation of a bound water molecule.

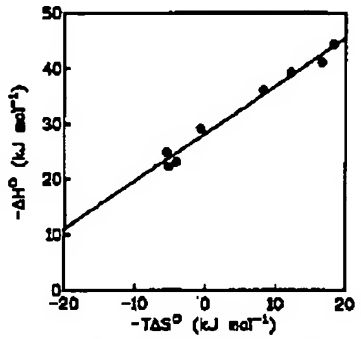

FIGURE 7: Enthalpy–entropy compensation plot for wild-type and mutant Se155-4 Fabs. The straight line was obtained by linear regression and has slope of 0.863 with an intercept of 28.3 kJ mol^{-1} ($r = 0.989$).

but possess many of the features of the periplasmic receptors, such as the aromatic residue stacking phenomenon and a reliance on hydrogen bonds. With respect to hydrogen-bond type, the carbohydrate recognition site of the Se155-4 antibody is somewhat unusual in that there is a lack of carboxylate and amide side-chain involvement in the hydrogen-bond network (Cygler et al., 1991). Instead, histidine side-chain, tryptophan side-chain, and backbone interactions dominate the hydrogen-bonding scheme. The stacking of aromatic side chains against the sugar ring is thought to discriminate against antigens carrying dideoxyhexoses other than abequose. Antigen mapping studies by functional group replacements (Bundle et al., unpublished results) have shown that the binding site fails to bind such antigens.

The His^{101H} mutagenesis results obtained for Se155-4 revealed that a number of interrelated factors are involved in the contribution of this residue to binding. The His^{101H}Glu and His^{101}Gln mutants displayed significantly higher enthalpy changes associated with trisaccharide binding. This is indicative of improved hydrogen-bond and/or van der Waals contacts. However, there was also a dramatic shift in the entropy term which more than offset the enthalpy gain. This result can be explained in different ways, but all point to the excellent balance between surface complementarity and hydrogen-bonding possibilities provided by the histidine side chain. The Glu and Gln substitutions may have resulted in the introduction of an additional hydrogen bond but the associated motional restrictions led to a net negative effect on affinity, because of a highly unfavorable entropy term. The formation of a bidentate hydrogen bond involving mannose and the Glu side chain is easily envisioned (Figure 6). Replacement of His^{101H} by dicarboxylic acids or the corresponding amides could potentially allow for simultaneous hydrogen bonding to both O-4 and O-6 of the mannose residue. Hydrogen bonding of this type has been observed in several carbohydrate–protein complexes and may require the participation of a bound water molecule acting as either a hydrogen-bond donor or acceptor (Vyas, 1991). Alternatively, the large negative entropy change could be the result of a loss of surface complementarity allowing one or more additional water molecules to be trapped in the complex. The thermodynamic behavior of His^{101H}Asn and His^{101H}Asp was similar to that of the wild type. The side chain of Asn can be superimposed on the imidazole ring of histidine so that the amido group occupies the same position as the π-N of the imidazole ring, whereas the equivalent amido group of Gln may be superimposed on the τ-N of the ring. These results offer evidence that the π-N of the histidine is the one that forms the hydrogen bond with O-4 mannose.

All of the His^{101H} mutants were characterized by an enthalpy–entropy compensation effect as shown by the linear relationship that exists for changes in the two terms for each mutant (Figure 7). Enthalpy–entropy compensation has previously been demonstrated in studies on the effects of the degree of ligand polymerization (Sigurskjold et al., 1991) and temperature (Sigurskjold & Bundle, 1992) on antigen binding by Se155-4. Strong enthalpy–entropy compensation has also been reported for three monoclonal anti-fluorescyl antibodies (Herron et al., 1986). Binding of the ligand by the wild type is predominantly enthalpy driven with some favorable assistance from entropy. This is somewhat atypical for sugar binding to proteins, where entropy is usually unfavorable. The source of the favorable entropy contribution is the efficient displacement of water molecules from the interacting surfaces of the protein binding site and the ligand. Changes in enthalpy and entropy always tend to compensate each other to some degree. For instance, if an enthalpic interaction is lost (e.g., a salt-bridge, a hydrogen bond, or a van der Waals interaction), an amount of entropy will be gained from this due to increased motional freedom and, conversely, increased motional restrictions will be introduced if a new binding interaction is formed. In aqueous solution, a substantial part of the enthalpy–entropy compensation comes from solvent displacement. When water molecules arrange themselves around the

surface of a solute (especially around hydrophobic surfaces), they form ordered structures with enthalpically stronger hydrogen bonds compensated by loss of entropy. When these molecules are stripped off upon binding, an amount of enthalpy is lost, compensated by an increase in entropy. If a group of analogous species interact by the same mechanism, then a linear relationship between enthalpy and entropy can be expected (Leffler & Grunwald, 1963). This linear relationship determines the extent of the compensation between $\Delta H°$ and $-T\Delta S°$. The Fab mutants described here all lie on the same line of compensation with a slope of 0.86. A slope of less than 1 (complete compensation) means that the free energy correlates with entropy; i.e., the binding becomes stronger as $-T\Delta S°$ becomes more negative. It follows from the van't Hoff relation, $\delta(\ln K)/\delta T = \Delta H°/(RT^2)$, that when $\Delta H° = 0$, the binding constant K is at its maximum. By extrapolation of the compensation plot, this occurs at $-T\Delta S° = \Delta G° = -32.8$ kJ mol^{-1}, which corresponds to $K = 5.0 \times 10^5$ M^{-1}. This K can be viewed as the maximum achievable for this particular ligand at 25 °C. It is seen that K for the wild type is reasonably close to this value but that it might be possible by further mutation to increase the affinity by a factor of 2. Interestingly, the highest K found in a study of the temperature dependence of ligand binding by Se155-4 was also 5.0×10^5 M^{-1}, occurring at 18 °C (Sigurskjold & Bundle, 1992).

An unusual number of the H3 residues of Se155-4 form backbone interactions with antigen. In the His^{101H}Gly mutant, the only H3 side-chain hydrogen bond to antigen was removed with surprisingly little effect on binding. A very favorable enthalpy term for this mutant suggested that a strong main-chain interaction had been introduced at position 101H. With this change, five of the nine H3 residues are glycine and four are contiguous in the sequence. This highly flexible structure should permit reorientation to allow a new interaction, and the unfavorable entropy term is consistent with this interpretation of the results. It is not possible, however, to exclude the explanation that the introduction of water-mediated hydrogen bonds accounts for the dramatically increased enthalpy contribution to binding. In either case, the data once again illustrate the enthalpy–entropy compensation effect (Figure 7) that may explain the difficulty in obtaining affinity increases in proteins already possessing good carbohydrate-binding properties (Vermersch et al., 1990, 1991). Gly^{102H} was found to be irreplaceable. Its backbone conformation is absolutely crucial because of the involvement of its NH in forming a hydrogen-bond network with the hydroxyl groups at *O*-2-abequose, *O*-2-galactose, and *O*-1-abequose. The frequent occurrence of Gly residues in CDR-H3s, as shown by reading frame preferences (Abergel & Claverie, 1991), is therefore not due entirely to their flexible nature but may reflect the roles of backbone H-bonding in antigen binding. Tyr^{103H}, a residue at the interface between the V_L and V_H domains, could be replaced only by alkyl/hydrophobic side chains, thus defining its role in the hydrophobic interaction between domains.

The CDR-H3 has a more complex origin than the other CDRs, deriving from the D-segment along with junctional and N-variability. It shows greater variability also as underlined by the Wu/Kabat plots of mouse H-chain variability (Wu & Kabat, 1970). These features point to this portion of the antibody combining site having greater importance in antigen recognition. The mutation data nevertheless show that binding activity is retained in a wide range of mutants with only one residue, Gly^{102H}, being irreplaceable. Thus, the natural process of somatic mutation in most cases would not result in loss of activity, and this robustness has obvious advantages in the efficiency of somatic mutations to produce affinity improvements.

The results presented here once again draw attention to the crucial role that framework residue Arg^{94H} (position 94H in the Kabat numbering system) can play in H3 conformation. Changes to this residue have altered the binding characteristics of anti-digoxin (Panka et al., 1988; Novotny et al., 1990) and anti-phosphorylcholine (Chien et al., 1989) antibodies. It is generally assumed that it exerts its structural role by formation of a salt-bridge with Asp^{106H} (position 101H in the Kabat numbering system). In support of this, Tempest et al. (1991) have observed that the grafting of a murine H3 from an antibody lacking arginine at this position was successful only if the arginine at this position in the human framework was substituted. It is clear that a positive charge at heavy-chain position 98 is an essential feature of Se155-4. The requirement for a negative charge at position 106H is less stringent, suggesting that the role of Arg^{94H} is not limited to the formation of the Arg^{94H}–Asp^{106H} salt-bridge. An understanding of how framework structure affects hypervariable loop conformation and of the atomic interactions between loop residues and bound antigen will form the basis of successful antibody engineering. For example, the humanizing of murine monoclonal antibodies by grafting murine CDRs on human frameworks will not work if loop conformation is distorted in the process; compatible frameworks must be identified or engineered (Foote & Winter, 1992).

The blocking of affinity increases by entropy effects and the influence of framework changes on antigen binding thermodynamics emphasize the limitations of predictive redesign of antibodies, even when three-dimensional details of antigen and antibody structure are known. The generation of random mutations, coupled with the emerging phage display technology that enables selection for rare mutants from huge libraries (Barbas et al., 1991; Marks et al., 1991; Narang et al., unpublished results), may be a preferred route for tailoring the binding properties of antibodies to meet different requirements.

ACKNOWLEDGMENT

We thank Dr. X. Ma for help with designing the mutagenesis strategy, Dr. Steve Evans for help with the stereo diagrams, and Mr. V. Tuli for technical assistance. NRCC no. 34296.

REFERENCES

Abergel, C., & Claverie, J.-M. (1991) *Eur. J. Immunol. 21*, 3021–3025.

Alt, F. W., & Baltimore, D. (1982) *Proc. Natl. Acad. Sci. U.S.A. 79*, 4118–4122.

Alzari, P. M., Lascombe, M.-B. & Poljak, R. J. (1988) *Annu. Rev. Immunol. 6*, 555–580.

Anand, N. N., Dubuc, G., Mandal, S., Phipps, J., Gidney, M. A. J., Sinnott, B., Young, N. M., MacKenzie, C. R., Bundle, D. R., & Narang, S. A. (1990) *Protein Eng. 3*, 541–546.

Anand, N. N., Dubuc, G., Phipps, J., MacKenzie, C. R., Sadowska, J., Young, N. M., Bundle, D. R., & Narang, S. A. (1991a) *Gene 100*, 39–44.

Anand, N. N., Mandal, S., MacKenzie, C. R., Sadowska, J., Sigurskjold, B., Young, N. M., Bundle, D. R., & Narang, S. A. (1991b) *J. Biol. Chem. 266*, 21874–21879.

Barbas, C. F., Kang, A. S., Lerner, R. A., & Benkovic, S. J. (1991) *Proc. Natl. Acad. Sci. U.S.A. 88*, 7978–7982.

Better, M., Chang, C. P., Robinson, R. R., & Horwitz, A. H. (1988) *Science 240*, 1041–1043.

Bundle, D. R., & Young, N. M. (1992) *Curr. Opin. Struct. Biol. 2*, 666–673.
Chien, N. C., Roberts, V. A., Ginsti, A. M., Scharff, M. D., & Getzoff, E. D. (1989) *Proc. Natl. Acad. Sci. U.S.A. 86*, 5532–5536.
Chothia, C., & Lesk, A. M. (1987) *J. Mol. Biol. 196*, 901–917.
Cygler, M., Rose, D. R., & Bundle, D. R. (1991) *Science 253*, 442–445.
Feizi, T. (1991) *Curr. Opin. Struct. Biol. 1*, 766–770.
Foote, J., & Winter, G. (1992) *J. Mol. Biol. 224*, 487–499.
Herron, J. N., Kranz, D. M., Jameson, D. M. & Voss, E. W. (1986) *Biochemistry 25*, 4602–4609.
Leffler, J. E., & Grunwald, E. (1963) *Rates and Equilibria of Organic Reactions*, Wiley, New York.
Marks, J. D., Hoogenboom, H. R., Bonnert, T. P., McCafferty, J., Griffiths, A. D., & Winter, G. (1991) *J. Mol. Biol. 222*, 581–597.
Mian, I. S., Bradwell, A. R., & Olson, A. J. (1991) *J. Mol. Biol. 217*, 133–151.
Narang, S. A., Yao, F. L., Michniewicz, J. J., Dubuc, G., Phippa, J., & Somorjai, R. L. (1987) *Protein Eng. 1*, 481–485.
Narang, S. A., Brummell, D. A., Sharma, V., Dubuc, G., MacKenzie, C. R., Michniewicz, J., Sadowska, J., Anand, N., Young, N. M., & Bundle, D. R. (1991) *Nucleic Acids Res. Symp. Ser. 24*, 173–179.
Novotny, J., Bruccoleri, R. E., & Haber, E. (1990) *Proteins: Struct., Funct. Genet. 7*, 93–98.
Panka, D. J., Mudgett-Hunter, M., Parks, D. R., Peterson, L. L., Herzenberg, L. A., Haber, E., & Marjolies, M. N. (1988) *Proc. Natl. Acad. Sci. U.S.A. 85*, 3080–3084.
Quiocho, F. A. (1991) *Curr. Opin. Struct. Biol. 1*, 922–933.
Sambrook, J., Fritsch, E. F., & Maniatis, T. (1989) *Molecular Cloning: A Laboratory Manual*, 2nd ed., Cold Spring Harbor Laboratory, Cold Spring Harbor, NY.
Sigurskjold, B. W., & Bundle, D. R. (1992) *J. Biol. Chem. 267*, 8371–8376.
Sigurskjold, B. W., Altman, E., & Bundle, D. R. (1991) *Eur. J. Biochem. 197*, 239–246.
Skerra, A., & Plückthun, A. (1988) *Science 240*, 1038–1040.
Spurlino, J. C., Lu, G.-Y., & Quiocho, F. A. (1991) *J. Biol. Chem. 266*, 5202–5219.
Svenson, S. B., & Lindberg, A. A. (1978) *J. Immunol. 120*, 1750–1758.
Takeo, K., & Kabat, E. A. (1978) *J. Immunol. 121*, 2305–2310.
Takeo, K., & Nakamura, S. (1972) *Arch. Biochem. Biophys. 153*, 1–7.
Tempest, P. R., Bremner, P., Lambert, M., Taylor, G., Furze, J. M., Carr, F. J., & Harris, W. J. (1991) *Bio/Technology 9*, 266–271.
Vermersch, P. S., Tesmer, J. J. G., Lemon, D. D., & Quiocho, F. A. (1990) *J. Biol. Chem. 265*, 16592–16603.
Vermersch, P. S., Lemon, D. D., Tesmer, J. J. G., & Quiocho, F. A. (1991) *Biochemistry 30*, 861–866.
Vyas, N. K. (1991) *Curr. Opin. Struct. Biol. 1*, 732–740.
Vyas, N. K., Vyas, M. N., & Quiocho, F. A. (1991) *J. Biol. Chem. 266*, 5226–5237.
Wiseman, T., Williston, S., Brandts, J. F., & Lin, L.-N. (1989) *Anal. Biochem. 17*, 131–137.
Wu, T. T., & Kabat, E. A. (1970) *J. Exp. Med. 132*, 211–250.

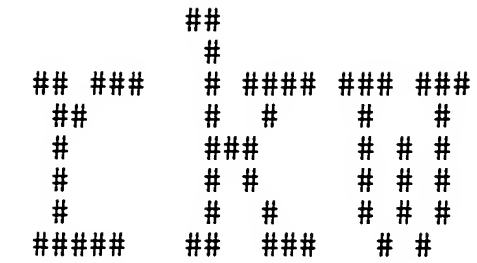

Job : 207
Date: 2/7/2007
Time: 1:05:12 PM

Protein Engineering vol.12 no.10 pp.879–884, 1999

Tryptophan H33 plays an important role in pyrimidine (6–4) pyrimidone photoproduct binding by a high-affinity antibody

Hiroyuki Kobayashi, Jiro Kato, Hiroshi Morioka, Jon D.Stewart[1] and Eiko Ohtsuka[2]

Graduate School of Pharmaceutical Sciences, Hokkaido University, Kita-ku, Sapporo 060-0812, Japan and [1]Department of Chemistry, University of Florida, Gainesville, FL 32611, USA

[2]To whom correspondence should be addressed; email: ohtsuka@pharm.hokudai.ac.jp

The importance of Trp H33 in antibody recognition of DNA containing a central pyrimidine (6–4) pyrimidone photoproduct was investigated. This residue was replaced by Tyr, Phe and Ala and the binding abilities of these mutants were determined by surface plasmon resonance and fluorescence spectroscopy. Conservative substitution of Trp H33 by Tyr or Phe resulted in moderate losses of binding affinity; however, replacement by Ala had a significantly larger impact. The fluorescence properties of DNA containing a (6–4) photoproduct were strongly affected by the identity of the H33 residue. DNA binding by both the wild-type and the W-H33-Y mutant was accompanied by a small degree of fluorescence quenching; by contrast, binding by the W-H33-F and W-H33-A mutants produced large fluorescence increases. Taken together, these variations in binding and fluorescence properties with the identity of the H33 residue are consistent with a role in photoproduct recognition by Trp H33 in the high-affinity antibody 64M5.

Keywords: antibodies/fluorescence/mutagenesis/pyrimidine (6–4) pyrimidone photoproduct/surface plasmon resonance

Introduction

Pyrimidine (6–4) pyrimidone dimers are major products of DNA photodamage that have been associated with mutation and cell death in the absence of repair (Friedberg *et al.*, 1995; Sancar, 1996; Wood, 1996). *In vivo*, (6–4) photoproducts are detected and corrected efficiently by enzymes of the excision repair pathway (Jones and Wood, 1993). Because they have very high binding affinities and specificities that can be programmed by proper choice of the immunogen, monoclonal antibodies have also been explored as a means to detect and quantitate these photolesions (Roza *et al.*, 1988; Mizuno *et al.*, 1991; Mori *et al.*, 1991; Matsunaga *et al.*, 1993). While the three-dimensional structures of antibodies and repair proteins are undoubtedly quite different, it is possible that both utilize similar features to distinguish photodamage lesions in the presence of a vast excess of normal B-helical DNA. We have therefore studied a series of murine monoclonal antibodies raised against UV-irradiated calf thymus DNA (Mori *et al.*, 1991). Four of these antibodies were specific for DNA containing pyrimidine (6–4) pyrimidone photoproducts in both single- and double-stranded DNA. The variable region genes for these four anti-(6–4) photoproduct antibodies have been cloned and sequenced (Morioka *et al.*, 1998). Three of the four sequences (antibodies 64M2, 64M3 and 64M5) are highly related to one another; however, the 64M5 antibody binds antigen at least an order of magnitude more tightly than the 64M2 and 64M3 antibodies (Mori *et al.*, 1991).

A variety of techniques have been used to examine the details of protein–DNA interactions in the series of anti-(6–4) photoproduct antibodies. Computer modeling predicted that the Fv structures of antibodies 64M2, 64M3 and 64M5 would be highly similar and that interactions with the (6–4) photoproduct itself would involve mainly non-charged interactions since the center of the combining site was predicted to possess few ionizable amino acid side chains (Morioka *et al.*, 1998). On the other hand, it was observed experimentally that the affinity of the 64M5 antibody for oligonucleotides containing a central (6–4) photoproduct increased with increasing lengths up to a hexanucleotide (Kobayashi *et al.*, 1998a). This suggests that electrostatic contacts might be formed between antibody side chains and phosphate groups on flanking regions of the oligonucleotides and these have been detected experimentally by ^{31}P NMR (Torizawa *et al.*, 1998). A strongly cationic patch was observed on the 64M5 VH surface approximately 20 Å from the center of the combining site. Single and multiple alanine replacements for the four lysine residues making up this cationic patch were created and the properties of these mutants suggested that the region functioned in the wild-type protein as an 'electrostatic steering' element during the association phase of DNA binding, although these amino acid side chains apparently did not interact directly with the antigen after binding had occurred (Kobayashi *et al.*, 1998b). Mutagenesis studies of CDR loop amino acids that differed between the 64M5 and 64M2 antibodies suggested that these proteins undergo conformational changes upon antigen binding and that the greater propensity to undergo these conformational changes is the major reason for the higher affinity of the 64M5 antibody (Kobayashi *et al.*, 1999). The X-ray crystal structures of the free 64M5 Fab fragment and the 64M2 Fab fragment complexed with a d(TT) (6–4) photoproduct dimer have been solved recently (Yokoyama,H., Mizutani,R., Satow,Y., Komatsu,Y., Ohtsuka,E. and Nikaido,O., manuscript in preparation). These experimental structures were very similar to those predicted by computer modeling and comparison of the bound and free states showed the conformational changes expected from earlier studies. The apparent stacking interaction between the Trp H33 side chain and the 3′ pyrimidone nucleotide was a particularly striking feature of the 64M2 complex structure (Figure 1). This Trp residue, located in VH CDR1, is conserved in the 64M2, 64M3 and 64M5 antibodies and also in a number of other murine anti-DNA antibodies of the γ2a and γ2b subclasses (Kabat *et al.*, 1992).

Stacking interactions between indole rings and nucleoside bases have been implicated in a variety of protein–DNA interactions. NMR studies have demonstrated such interactions with undamaged DNA in both model peptides (Sartorius and Schneider, 1995) and the HIV capsid protein (Morellet *et al.*,

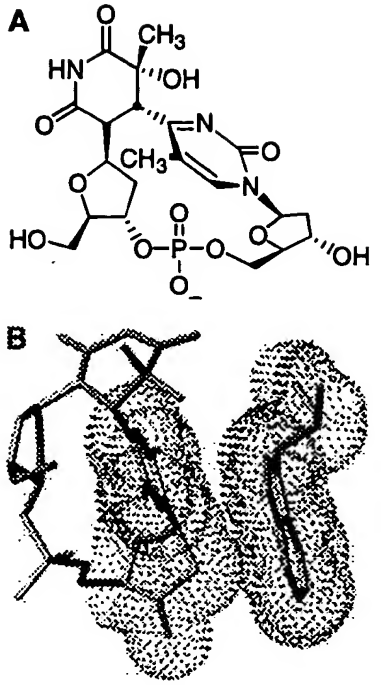

Fig. 1. Pyrimidine (6–4) pyrimidone photoproduct and its interaction with the 64M2 antibody. (**A**) Structure of the d(TT) (6–4) photoproduct. (**B**) Contact between the 64M2 Trp H33 side chain and the 3′ pyrimidone of the bound (6–4) photodimer. These coordinates were taken from the X-ray structure of this complex, which was prepared by co-crystallization with the photodimer shown in (A). Heavy atoms of both the protein and DNA are shown as heavy gray lines and the van der Waals surface of both Trp H33 and the pyrimidone portion of the photoproduct are indicated by black dots.

1998). These interactions have also been observed in damaged DNA recognition. Pi-stacking interactions between indole and methylated adenine derivatives have been investigated by small-molecule X-ray crystallography (Isbida *et al.*, 1983; Yamagata *et al.*, 1994) as models for the repair enzyme 3-methyladenine DNA glycosylase, whose crystal structure in a complex with DNA has been recently determined (Lau *et al.*, 1998). A π-stacking role for a tryptophan side chain has also been proposed for *Escherichia coli* exonuclease III (AP endonuclease VI) (Shida *et al.*, 1996).

In this paper, we examine the role of Trp H33 in photoproduct binding by the 64M5 scFv. Mutants were constructed in which this residue was substituted with phenylalanine, tyrosine or alanine. While the W-H33-F and W-H33-Y mutants retained a large fraction of the wild-type binding affinity for DNA's containing a (6–4) photoproduct, the W-H33-A substitution dramatically diminished antigen binding. Pyrimidine (6–4) pyrimidone photoproducts are fluorescent, and this property was exploited to probe the local environment of the bound antigen in the wild-type and the mutant scFvs. Taken together, our results indicate that Trp H33 plays a key role in DNA photoproduct binding by the 64M5 antibody, most likely by π-stacking interactions.

Materials and methods

General

Restriction and DNA modifying enzymes were purchased from Takara Shuzo, New England Biolabs, Bethesda Research Labs, Stratagene, Toyobo or Boehringer Mannheim. Reagents were obtained from Wako Pure Chemical Industries, Nacalai Tesque or Sigma Chemical and were used as received. DNA phosphoramidite reagents were obtained from Perkin Elmer Applied Biosystems. Routine cloning was performed according to Sambrook *et al.* (1989).

Preparation of oligonucleotides

Solid-phase oligonucleotide synthesis was carried out on an Applied Biosystems Model 394 DNA/RNA synthesizer using standard β-cyanoethyl chemistry according to the manufacturer's protocol. Oligonucleotides were purified for surface plasmon resonance measurements by reversed-phase HPLC (μBondapak C18, Waters). Those used for molecular biology techniques were purified by denaturing polyacrylamide gels. 3′-Biotinylated oligonucleotides containing a (6–4) photoproduct (T[6–4]T and CAAT[6–4]TAAG) were prepared as described previously (Kobayashi *et al.*, 1998a).

Production and isolation of mutant 64M5 scFv's

Trp H33 was replaced by alanine, phenylalanine and tyrosine using PCR methods (Higuchi, 1989) and detailed procedures have been described previously (Kobayashi *et al.*, 1999). All mutant DNA sequences were confirmed by automated DNA sequencing (Applied Biosystems Model 373A). Once constructed, each mutant scFv gene was introduced into an expression plasmid in which the scFv was fused to a hexahistidine tag (Kobayashi *et al.*, 1999).

All of the scFv's accumulated in *Escherichia coli* cells in the form of inclusion bodies according to SDS–PAGE and western blotting. Active proteins were obtained by solubilizing the inclusion bodies in 6 M guanidinium hydrochloride followed by an on-column refolding and purification procedure (Kobayashi *et al.*, 1999). The scFv's were further purified by gel filtration using a Superose 12 HR 10/30 column equilibrated with HBS (10 mM HEPES, pH 7.4, 150 mM NaCl, 3.4 mM EDTA, 0.005% Tween-20) using a SMART-system (Pharmacia Biotech).

Surface plasmon resonance determination of (6–4) photoproduct binding by scFv's

Binding of scFv's to oligonucleotides containing a (6–4) photoproduct was measured by surface plasmon resonance (SPR) measurements using a BIAcore instrument as described previously (Kobayashi *et al.*, 1999). The minimal amount of DNA was immobilized on the sensor chip in order to avoid mass transport limitations. Injections of biotinylated oligonucleotides (0.01 pmol/μl in HBS) were repeated until the SPR signal was increased by 10–30 resonance units (RU) above the original baseline. Purified scFv's were diluted in HBS buffer, then they were injected over the immobilized oligonucleotides at a flow rate of 100 μl/min over a concentration range from 10 to 200 nM. Sensorgrams were recorded and normalized to a base line of 0 RU. Equivalent volumes of diluted antibodies were also injected over a non-oligonucleotide surface to serve as blank sensorgrams to allow subtraction of the bulk refractive index background. The association was monitored by measuring the rate of binding to antigen at different protein concentrations. The dissociation of these antibodies from the antigen surface was monitored after the end of the association phase. The remaining bound antibodies were removed completely by injecting 50–100 μl 100 mM HCl. Kinetic rate constants were calculated using BIAevaluation 2.1 software (Biacore) using a single-site binding model (A + B = AB). The ratio of the

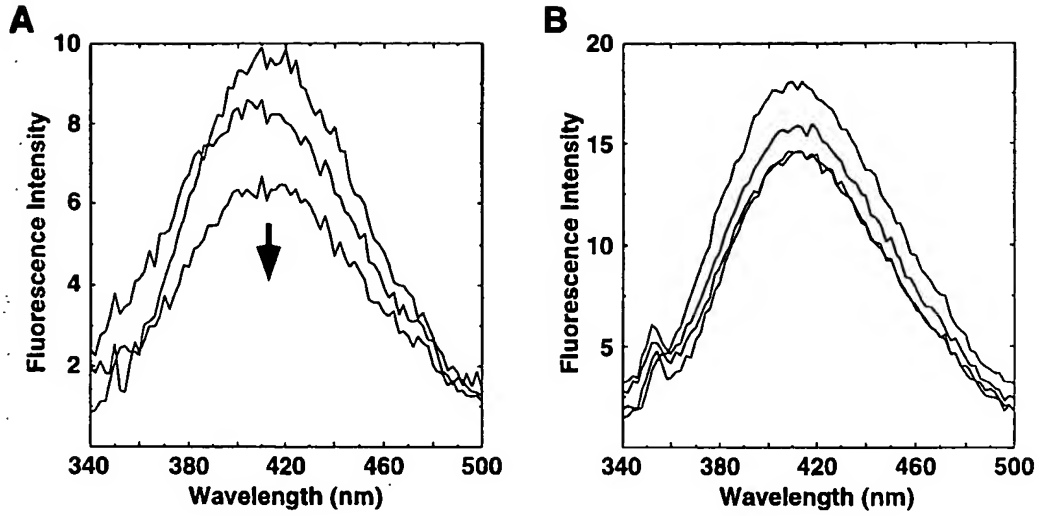

Fig. 2. Fluorescence emission spectra of the (6–4) photoproduct with excitation at 313 nm in the presence of wild-type 64M5 scFv. (A) Emission spectrum of 200 pmol [5′-d(CAAT(6–4)TAAG)-3′] in the presence of 0, 100 and 200 pmol wild-type 64M5 scFv. (B) Emission spectrum of 50 pmol [5′-d(T(6–4)T)-3′] in the presence of 0, 25, 50 and 100 pmol wild-type 64M5 scFv. No clear trend in intensity changes as a function of added scFv was observed in this case.

Table I. Kinetic constants for the binding of scFv's to oligonucleotides containing a (6–4) photoproduct

scFv	d2-mer-(6–4)[a]			d8-mer-(6–4)[b]		
	k_{ass} ($M^{-1}s^{-1}$)	k_{diss} (s^{-1})	k_{diss}/k_{ass} (M)	k_{ass} ($M^{-1}s^{-1}$)	k_{diss} (s^{-1})	k_{diss}/k_{ass} (M)
Wild type[c]	$(9.5\pm0.7)\times10^{5}$	$(1.5\pm0.2)\times10^{-3}$	$1.6\pm0.2)\times10^{-9}$	$(1.1\pm0.1)\times10^{6}$	$(1.1\pm0.2)\times10^{-4}$	$(1.0\pm0.1)\times10^{-10}$
W-H33-Y	$(9.0\pm0.1)\times10^{4}$	$(4.4\pm0.4)\times10^{-3}$	$(4.9\pm0.4)\times10^{-8}$	$(4.8\pm0.3)\times10^{5}$	$(2.1\pm0.1)\times10^{-4}$	$(4.4\pm0.3)\times10^{-10}$
W-H33-F	$(1.9\pm0.3)\times10^{4}$	$(8.4\pm0.3)\times10^{-3}$	$(4.4\pm0.7)\times10^{-7}$	$(4.5\pm0.1)\times10^{5}$	$(2.1\pm0.1)\times10^{-4}$	$(4.7\pm0.2)\times10^{-10}$
W-H33-A	ND	ND	–	$(1.3\pm0.6)\times10^{5}$	$(1.0\pm0.1)\times10^{-2}$	$(8.0\pm4.0)\times10^{-8}$

[a]d(T<6–4>T).
[b]d(CAAT<6–4>TAAG).
[c]Kobayashi *et al.* (1999).
ND, No binding detected under standard conditions.

rate constants allowed the apparent equilibrium constant to be calculated, $K_{D,app} = k_{diss}/k_{ass}$.

Fluorescence measurements of (6–4) photoproduct with scFv's

Steady-state fluorescence excitation and emission spectra of (6–4) photoproduct with scFv's were measured on a Model FP-777 spectrofluorometer (Japan Spectroscopic Co, Ltd) using a 6 mm square cuvette and a sample volume of 200 µl. The emission spectra were recorded over the wavelength range from 250 to 500 nm with an excitation wavelength of 313 nm. The spectral bandpass was 5 nm for all emission spectra. After obtaining the emission scan for the photoproduct-containing oligonucleotides alone in a HBS buffer, scFv proteins were added at the indicated concentrations and allowed to equilibrate for 30 min at 25°C prior to spectral measurements.

Results

A tryptophan at position H33 is present in all three closely-related anti-(6–4) photoproduct antibodies (64M2, 64M3 and 64M5). Moreover, the three-dimensional structures of the 64M2 and 64M5 Fab fragments determined by X-ray crystallography are highly similar (Yokoyama,H., Mizutani,R., Satow,Y., Komatsu,Y., Ohtsuka,E. and Nikaido,O., manuscript in preparation). We therefore chose to investigate the role of Trp H33 in the context of the 64M5 scFv since this antibody has the highest affinity for photoproduct-containing oligonucleotides (Mori *et al.*, 1991) and because of our previous experience in site-directed mutagenesis studies of the 64M5 scFv (Kobayashi *et al.*, 1998b, 1999). We expect the role of Trp H33 to be identical in antigen binding by the 64M2, 64M3 and 64M5 antibodies. All scFv's used in this study had the VL–linker–VH–His_6 structure that better reproduces the binding properties of the native 64M5 monoclonal antibody and the proteolytically-prepared Fab fragment (Kobayashi *et al.*, 1999).

We replaced Trp H33 by Ala, Phe and Tyr using standard site-directed mutagenesis techniques (Higuchi, 1989) and expressed the scFv proteins along with C-terminal hexahistidine tags in *E.coli* as inclusion bodies. The pure scFv proteins were prepared by solubilizing the inclusion bodies with denaturant, capturing the unfolded proteins on metal affinity columns, then re-folding the scFv proteins while still attached to the solid support (Kobayashi *et al.*, 1999). After elution from the metal affinity column, the scFv's were further purified by gel filtration chromatography. The final chromatography step also indicated that the wild-type and all three mutant scFv's were predominantly monomeric under the experimental conditions.

The rate constants for photoproduct binding by the scFv's were determined by surface plasmon resonance and the data are summarized in Table I. Two DNA's were used: the (6–4) photodimer and an octanucleotide that contained a central

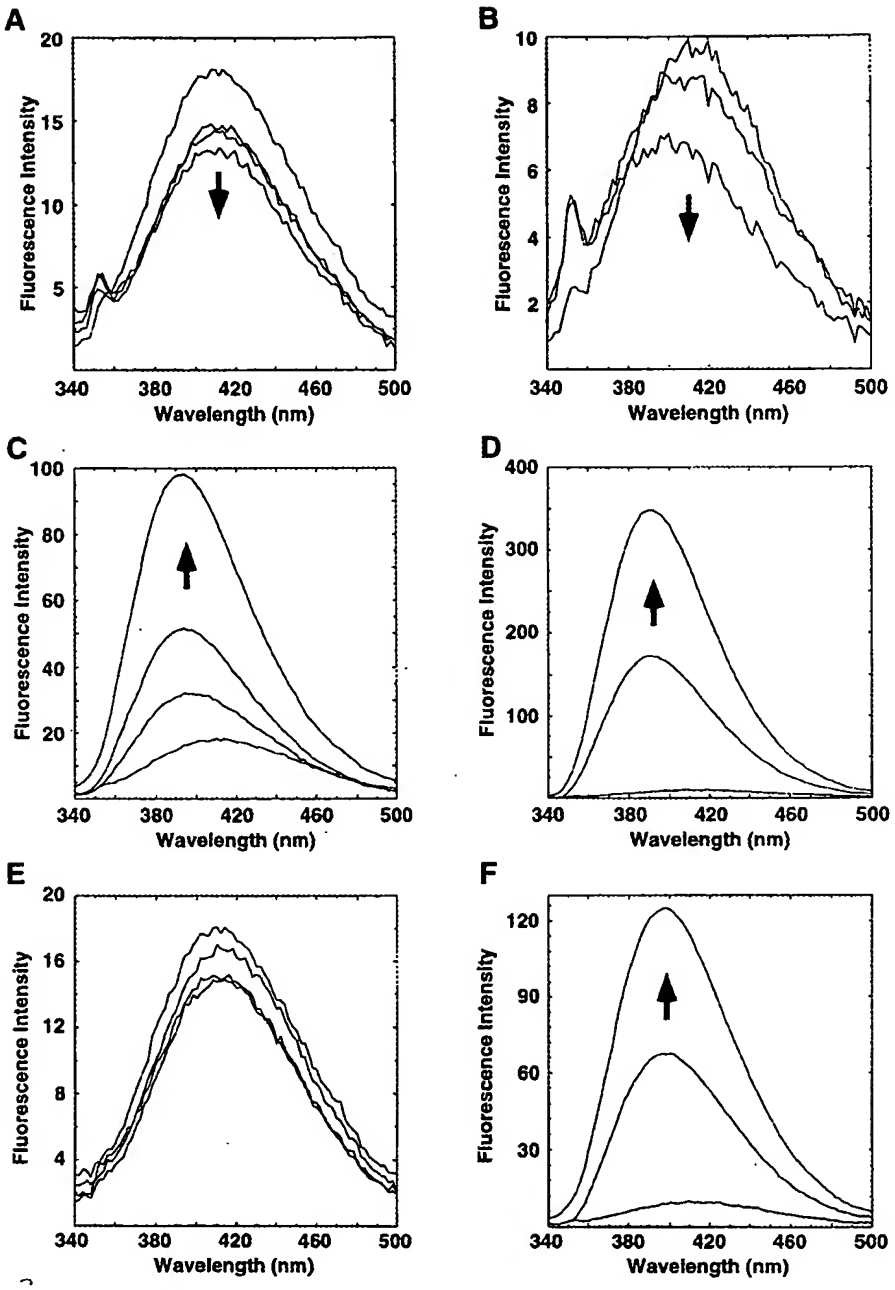

Fig. 3. Fluorescence emission spectra of the (6–4) photoproduct with excitation at 313 nm in the presence of mutant 64M5 scFv's. When observable, trends in intensity changes as a function of added scFv are indicated by arrows. (A) Emission spectrum of 50 pmol [5′-d(T(6–4)T)-3′] in the presence of 0, 25, 50 and 100 pmol W-H33-Y 64M5 scFv. (B) Emission spectrum of 200 pmol [5′-d(CAAT(6–4)TAAG)-3′] in the presence of 0, 100 and 200 pmol W-H33-Y 64M5 scFv. (C) Emission spectrum of 50 pmol [5′-d(T(6–4)T)-3′] in the presence of 0, 25, 50 and 100 pmol W-H33-F 64M5 scFv. (D) Emission spectrum of 200 pmol [5′-d(CAAT(6–4)TAAG)-3′] in the presence of 0, 100 and 200 pmol W-H33-F 64M5 scFv. (E) Emission spectrum of 50 pmol [5′-d(T(6–4)T)-3′] in the presence of 0, 25, 50 and 100 pmol W-H33-A 64M5 scFv. (F) Emission spectrum of 200 pmol [5′-d(CAAT(6–4)TAAG)-3′] in the presence of 0, 100 and 200 pmol W-H33-A 64M5 scFv.

(6–4) photoproduct. The former was designed to probe interactions with the photoproduct itself while the latter would also allow contributions to binding energy by contacts with flanking nucleotides. The W-H33-A mutant was unable to bind the dimer at detectable levels under our experimental conditions, although binding to the octamer was measurable.

The (6–4) photoproduct fluoresces with an emission maximum near 405 nm when excited at 313 nm (Hauswirth and Wang, 1977; Franklin *et al.*, 1982). Because the fluorescence properties depend on the relative torsional angle between the 5′-pyrimidine and the 3′-pyrimidone ring of the photoproduct, we exploited this technique to characterize DNA binding by the 64M5 scFv mutants. Figure 2 shows the emission spectra of the (6–4) photoproduct dimer and octamer used previously to characterize the scFv's by surface plasmon resonance. Stepwise addition of the wild-type 64M5 scFv caused a small

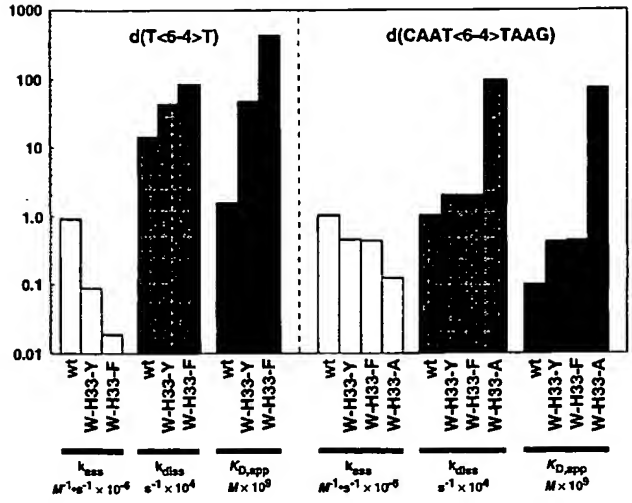

Fig. 4. Graphical representation of rate constants for photoproduct binding as determined by surface plasmon resonance.

progressive decrease in fluorescence intensity in the case of the octamer; however, only very slight changes were observed in the case of the dimer and no trend was apparent. In the case of the octamer, infinitely tight binding would be expected under the experimental conditions and the extent of fluorescence quenching as a function of added scFv was consistent with this expectation. Repeating this experiment with the W-H33-Y mutant gave similar results (Figure 3A and B). In the case of the octamer, infinitely tight binding was expected on the basis of the $K_{D,app}$ value determined by surface plasmon resonance and the data fit this expectation. In the case of the photoproduct dimer, both the DNA and the scFv concentrations were within an order of magnitude of the $K_{D,app}$ value. These data could be well described by a quadratic binding equation that incorporated the $K_{D,app}$ value determined by surface plasmon resonance (data not shown), demonstrating that both methods for detecting scFv–DNA interactions yielded consistent results and that the observed fluorescence changes are unlikely to be experimental artifacts.

When photodimer fluorescence spectra were determined in the presence of increasing concentrations of the W-H33-F mutant, large increases in fluorescence intensities were observed along with a pronounced blue shift (Figure 3C and D). Similar behavior was observed for the W-H33-A mutant (Figure 3F). These data were also consistent with quadratic binding equations incorporating $K_{D,app}$ values determined by surface plasmon resonance. Only small fluorescence changes were detected when the W-H33-A mutant was added to the (6–4) photodimer (Figure 3E), consistent with our inability to detect this interaction by surface plasmon resonance.

Discussion

While Trp commonly occurs at position H33 in anti-DNA antibodies, and it is conserved among all three closely-related anti-(6–4) photoproduct antibodies, a variety of other residues are also found in the Kabat database at this location including Ala, Phe and Tyr (Kabat *et al.*, 1992). All three H33 mutants retained the ability to bind (6–4) photoproduct-containing DNA, suggesting that the mutations did not drastically alter the native three-dimensional structure. The rate constants for (6–4) photoproduct binding by the wild-type and mutant scFv's are shown graphically in Figure 4. As would be expected for a residue that interacts strongly with the photoproduct itself, mutations of Trp H33 had the greatest impact on binding of the photodimer. The flanking nucleotides present in the octamer provide additional contacts independent of Trp H33 (Morioka *et al.*, 1998), and this reduces the impacts of all but the Ala mutation. The latter may be a special case, however, since the dramatic reduction in side chain volume may also affect the positioning of other nearby residues.

The energetic impact of removing Trp H33 on DNA binding is consistent with its proposed role in stacking with the photoproduct 3′-pyrimidone base and with the results of site-directed mutagenesis studies of Trp–DNA interactions in other proteins. For example, Voss and co-workers analyzed the consequences of mutating Trp H100A in anti-single-stranded DNA autoantibody BV04-01, whose side-chain had been shown by X-ray crystallography to stack against the central thymine base of bound $d(T_3)$ (Rumbley *et al.*, 1993). The role and positioning of this residue is thus analogous to that of Trp H33 in our photoproduct antibodies. Substitution of Trp H100A in BV04-01 by Tyr or Phe led to decreases in K_D values of 22- and 44-fold, respectively (Rumbley *et al.*, 1993). The corresponding alterations in $K_{D,app}$ values for mutation of Trp H33 to Tyr and Phe in 64M5 are 31- and 280-fold, respectively. In the case of DNA repair protein *E.coli* photolyase, a tryptophan side chain (Trp 277) is positioned within the substrate binding pocket (Park *et al.*, 1995). While mutation of this residue to Phe or His had little effect on substrate binding, replacement by His or Arg diminished the affinity of the protein by 1000-fold (Li and Sancar, 1990).

The alterations in (6–4) photoproduct fluorescence properties with changes in the H33 residue are also consistent with a π-stacking interaction involving Trp H33. Each mutation was introduced into the X-ray crystal structure of the 64M5 scFv using computer modeling. Interestingly, the aromatic rings of both Tyr and Phe were predicted to overlap with the 3′-pyrimidone base more extensively than the indole side chain of Trp H33. While it is not possible to quantitatively interpret the fluorescence changes caused by the 64M5 scFv, we note that the decrease in (6–4) photoproduct fluorescence intensity caused by the wild type 64M5 scFv was identical to that observed for the proteolytically-prepared 64M5 Fab (data not shown), suggesting that this quenching is an intrinsic part of the binding interaction rather than an artifact of the scFv. However, we cannot determine whether these changes in fluorescence properties are due to changes in the relative angle between the pyrimidine and pyrimidone π-systems upon binding, resonance energy transfer to nearby π-systems or some other mechanism. It is clear that replacing Trp H33 with Phe or Ala alters the local environment of the (6–4) photodimer since binding is accompanied by large fluorescence increases that are not seen with the wild-type scFv.

In summary, the results of the present study argue that Trp H33 plays a key role in (6–4) photoproduct binding by the high-affinity 64M5 antibody. Whether enzymes that recognize and repair these photolesions will also utilize a similar interaction with the 3′-pyrimidone base remains to be determined.

Acknowledgements

We thank Dr Yoshinori Satow (University of Tokyo) for permission to use the coordinates of the crystal structures cited in this work and Drs Yasuo Komatsu (Hokkaido University), Koichi Kato (University of Tokyo) and Ichio Shimada (University of Tokyo) for valuable discussions. This work was

supported by Grants-in-Aid by the Monbusho International Scientific Research Program and by Specially Promoted Research funding from the Ministry of Education, Science, Culture and Sports of Japan.

References

Franklin,W.A., Lo,K.M. and Haseltine,W.A. (1982) *J. Biol. Chem.*, **257**, 13535–13543.

Friedberg,E.C., Walker,G.C. and Siede,W. (1995) In *DNA Repair and Mutagenesis*. ASM Press, Washington, DC.

Hauswirth,W., and Wang,S.Y. (1977) *Photochem. Photobiol.*, **25**, 161–166.

Higuchi,R. (1989) In Erlich,H.A. (ed.), *PCR Technology*. Stockton Press, New York, pp. 61–70.

Ishida,T., Shibata,M., Fujii,K. and Inoue,M. (1983) *Biochemistry*, **22**, 3571–3581.

Jones,C.J. and Wood,R.D. (1993) *Biochemistry*, **32**, 12096–12104.

Kabat,E.A., Wu,T.T., Perry,H.M., Gottesman,K.S. and Foeller,C. (1992) *Sequences of Proteins of Immunological Interest*, Release 5.0. National Institutes of Health, Bethesda, MD. The most up-to-date release can be found at http://www.immuno.bme.nwu.edu

Kobayashi,H., Morioka,H., Torizawa,T., Kato,K., Shimada,I., Nikaido,O. and Ohtsuka,E. (1998a) *J. Biochem.*, **123**, 182–188.

Kobayashi,H., Morioka,H., Nikaido,O., Stewart,J.D. and Ohtsuka,E. (1998b) *Protein Engng*, **11**, 1089–1092.

Kobayashi,H., Morioka,H., Tobisawa,K., Torizawa,T., Kato,K., Shimada,I., Nikaido,O., Stewart,J.D. and Ohtsuka,E. (1999) *Biochemistry*, **38**, 532–539.

Lau,A.Y., Scharer,O.D., Samson,L., Verdine,G.L. and Ellenberger,E. (1998) *Cell*, **95**, 249–258.

Li,Y.F. and Sancar,A. (1990) *Biochemistry*, **29**, 5698–5706.

Matsunaga,T., Hatakeyama,Y., Ohta,M., Mori,T. and Nikaido,O. (1993) *Photochem. Photobiol.*, **57**, 934–940.

Mizuno,T., Matsunaga,T., Ihara,M. and Nikaido,O. (1991) *Mutat. Res.*, **254**, 175–184.

Morellet,N., Demene,H., Teilleux,V., Huynh-Dinh,T., de Rocquigny,H., Fournie-Zaluski,M.C. and Roques,B.P. (1998) *J. Mol. Biol.*, **283**, 419–434.

Mori,T., Nakane,M., Hattori,T., Matsunaga,M., Ihara,M. and Nikaido,O. (1991) *Photochem. Photobiol.*, **54**, 225–232.

Morioka,H., Miura,H., Kobayashi,H., Koizumi,T., Fujii,K., Asano,K., Matsunaga,T., Nikaido,O., Stewart,J.D. and Ohtsuka,E. (1998) *Biochim. Biophys. Acta*, **1385**, 17–32.

Park,H.-W., Kim,S.-T., Sancar,A. and Deisenhofer,J. (1995) *Science*, **268**, 1866–1872.

Roza,L., Van der Wulp,K.J.M., Macfarlane,S.J., Lohman,P.H.M. and Baan,R.A. (1988) *Photochem. Photobiol.*, **48**, 627–633.

Rumbley,C.A., Denzin,L.K., Yanta,L., Tetin,S.Y. and Voss,E.W.,Jr (1993) *J. Biol. Chem.*, **268**, 13667–13674.

Sambrook,J., Fritsch,E.F. and Maniatis,T. (1989) *Molecular Cloning: A Laboratory Manual*, 2nd Edn. Cold Spring Harbor Laboratory Press, Cold Spring Harbor.

Sancar,A. (1996) *Annu. Rev. Biochem.*, **65**, 43–81.

Sartorius,J. and Schneider,H.J. (1995) *FEBS Lett.*, **374**, 387–392.

Shida,T., Noda,M. and Sekiguchi,J. (1996) *Nucleic Acids Res.*, **24**, 4572–4576.

Torizawa,T., Kato,K., Kimura,Y., Asada,T., Kobayashi,H., Komatsu,Y., Morioka,H., Nikaido,O., Ohtsuka,E. and Shimada,I. (1998) *FEBS Lett.*, **429**, 157–161.

Wood,R.D. (1996) *Annu. Rev. Biochem.*, **65**, 135–167.

Yamagata,Y., Kato,M. and Fujii,S. (1994) *Chem. Pharm. Bull.*, **42**, 2385–2387.

Received February 26, 1999; revised May 24, 1999; accepted June 21, 1999